Tetrahedron 64 (2008) 6230–6237

Contents lists available at ScienceDirect

Tetrahedron

journal homepage: www.elsevier.com/locate/tet

The influence of isomerism on the self-assembly behavior and complexation property of 1,3-alternate tetraaminopyridyl-thiacalix[4]arene derivatives

Xiong Li [a], Shu-Ling Gong [a,*], Wei-Ping Yang [a], Yuan-Yin Chen [a], Xiang-Gao Meng [b]

[a] College of Chemistry and Molecular Sciences, Wuhan University, Wuhan 430072, PR China
[b] College of Chemistry, Huazhong Normal University, Wuhan 430079, PR China

ARTICLE INFO

Article history:
Received 19 January 2008
Received in revised form 25 April 2008
Accepted 29 April 2008
Available online 1 May 2008

Keywords:
Thiacalixarene
Isomer
Self-assembly
Complexation

ABSTRACT

A series of 1,3-alternate conformation thiacalix[4]arenes containing different isomeric aminopyridyl pendent arms have been synthesized. It was found that their self-assembly behaviors and complexation properties strongly depended on the structures of aminopyridyl pendent arms. The crystal structures demonstrate that tetra(*meta*-aminopyridyl)-thiacalix[4]arene motif is capable of forming intramolecular hydrogen bondings between the sp^2 nitrogen donors in the *meta* position of the aminopyridyl groups and the facing amide N–H of the adjacent aminopyridyl groups, and self-assembles via C–H···O weak hydrogen bondings and C–H···π interaction to generate a double stranded rectilineal networks. By contrast, in the case of tetra(*para*-aminopyridyl)-thiacalix[4]arene, the presence of *para*-aminopyridyl units enables the formation of N–H···N strong hydrogen bondings between the individual molecules leading to the solid-state structure with water-bridged double strands. Their complexation properties had been also studied by measurement of the stability constants for their complexation in a range of metal cations and investigation of their binding models via ^{1}H NMR titration and ESI-MS experiments. It was found that the three ligands exhibited high and selective extractability toward Ag^+, and their stoichiometry of ligand to Ag^+ was 1:1, while the *meta*-aminopyridyl derivative showed the best extraction capacity and possessed the most efficient binding sites.

© 2008 Elsevier Ltd. All rights reserved.

1. Introduction

Calixarenes[1,2] are synthetic macrocycles derived from the condensation of phenols and formaldehyde, which, depending on the number of aromatic units in the cyclic array and on the functionalization at the phenolic oxygen atoms (lower or narrow rim), have been actively studied and utilized as the third generation of host compounds in addition to the well-known crown ethers[3] and cyclodextrins.[4] The introduction of suitable donor groups at the lower rim of calixarenes produces powerful and selective ionophores, particularly for spherical metal ions.[5] Extensively studied are the calix[4]arene podands and the calix[4]crowns showing high efficiency and selectivity toward silver metal[6,7] due to its considerable utility of the noble metal in the fields of anti-bacterial medicine, catalysis, optoelectronics, microelectronics, and so on.[8] The binding ability of the most Ag^+ ionophores is based alike on the preferred interaction between the soft Ag^+ ion and the donor atoms such as N.

Although the complexation of metal ions continues to occupy a central place in calixarene chemistry,[1–3] more recent attention has also been devoted to the self-assembly of calixarene building blocks into solid-state supramolecular architectures, which are currently investigated extensively in the fields of chemical, biological, and materials science and technology.[2] One of the most important features of these supramolecular architectures is the simultaneous operation of several cooperative weak forces working between molecular building blocks or tectons[9] such as van der Waals, electrostatic, π–π, CH–π, H-bonding, coordination bonding, etc.[10–12] Among the various types of molecular tectonics, the calixarenes adorned with hydrogen bonding donor and acceptor groups at the upper rim or the lower rim are particularly attractive,[12,13] since they can act as building blocks for the noncovalent synthesis of nanostructures,[14] ion channels,[15] self-assembled dimeric capsules, and so on.[16–18]

In the crystalline phase, molecular networks are defined by the nature of tectons composing the architecture (shape, interaction sites, and their localization in space), the type of interaction involved in the interconnection of consecutive tectons, and finally, the number of independent translations operating on the recognition patterns.[19,20] Thus, one strategy that has been used to modulate the self-assembly behavior is to alter the localization of interaction sites in the organic tecton. In other terms, one must take into account the influence of isomerism of the interaction sites on the self-assembly behavior and design the organic tecton accordingly. There are few examples with this aspect, most notably,

* Corresponding author. Fax: +86 27 68754067.
E-mail address: gongsl@whu.edu.cn (S.-L. Gong).

0040-4020/$ – see front matter © 2008 Elsevier Ltd. All rights reserved.
doi:10.1016/j.tet.2008.04.116

Pansanel and co-worker[20] reported that two organic tectons, based on a 1,4-phenylenediamine backbone functionalized with two isomeric pyridine units through amide junctions, self-assemble in the presence of $HgCl_2$ to generate two types of 2-D networks, one of the purely metallo-organic type, based on only coordination bonds, and the other combining both coordination and hydrogen bonds.

Thiacalix[4]arenes, in which the four methylene bridges of 'usual' calix[4]arenes are replaced by sulfur,[21] have a slightly different size and shape.[22] Therefore, thiacalix[4]arene derivatives have (eventually significantly) different complexation properties[23] and different self-assembly preferences.[18] Herein, we report the synthesis of thiacalix[4]arene analogs **4a**–**c** in 1,3-alternate conformation comprising O and N ligating sites by anchoring isomeric amidopyridyl groups to the lower rim and the effect of the amidopyridyl side chain's substitution pattern on their metal ion-binding properties. In addition, the presence of aminopyridyl groups in an alternating mode below and above its main plane provides additional hydrogen bond donors and acceptors, facilitating the formation of a H-bonding supramolecular assembly. In this paper, we also demonstrate the solid-state structural analysis of the free ligands differing only by the position of connection of the amide group to the pyridyl group (*meta* for **4b** and *para* for **4c**) and of two completely different types of 1-D supramolecular self-assembled systems, especially, the analogous thiacalix[4]arene **4c** self-assembles to form ordered arrays containing water-bridged double strands. By comparing ion-binding and self-assembly properties of isomers **4a**–**c**, we find that the amidopyridyl's substitution pattern is essential for mediating ion-binding and self-assembly network.

2. Results and discussion

2.1. Synthesis and structural assignments

As illustrated in Scheme 1, the synthesis started from parent thiacalix[4]arene, which was transformed into the corresponding tetraacetate in 1,3-alternate conformation by alkylation with ethyl bromoacetate in refluxing acetone using Cs_2CO_3 as a base according to the known procedures.[24] The corresponding acid chloride was prepared by hydrolysis of ester with aq NaOH in a mixture of ethanol and water,[25] followed by treatment with thionyl chloride in refluxing CH_2Cl_2 for 48 h in good yield. The crude chloride was used without purification for subsequent condensation with the aminopyridine isomers, and the corresponding tetraamides were obtained in high yields. In order to explore the complexation behavior of ligands, the correlative reference compounds **7a**–**c** were also synthesized from *p*-*tert*-butyl-phenol as shown in Scheme 1.

Structures of the above-mentioned thiacalix[4]arene derivatives **4a**–**c** were proved by the combination of ^{1}H NMR spectroscopy and mass spectroscopy (ESI-MS). The ESI-MS spectra of all receptors **4a**–**c** showed the only one most intense signals corresponding to the molecular peak [MH^+] (100% int.), which showed that they were tetraaminopyridine products. All their ^{1}H NMR spectra showed a singlet for the *tert*-butyl groups, a singlet for the aromatic protons and a singlet for OCH_2CO, which precisely reflected its S_4 symmetry. It is obvious that all the compounds adopted 1,3-alternate conformation or cone conformation. It was reported that both in the calix[4]arene and thiacalix[4]arene bearing ester functional groups, the chemical shift of the *tert*-butyl protons in the cone conformation are located at higher field than that in the 1,3-alternate conformation. The signal of *tert*-butyl protons of **4a**–**c** appears at δ 0.70–0.80 ppm, which is at much higher field than the chemical shift of the *tert*-butyl protons either in the 1,3-alternate conformation (approximately δ 1.25 ppm) or in the cone conformation (usually >1.00 ppm),[7,24–27] the large highfield shift indicates that the *tert*-butyl protons are exposed to the ring current shielding effect operating in the proximal pyridine ring. The result is explicable only by the steric characteristics of 1,3-alternate conformation that the four *tert*-butyl and four pyridine groups are symmetrically distributed on the two side of thiacalixarene cavity so that the *tert*-butyl protons can locate at the shielding field of the pyridine ring. Moreover, the synthetic pathway started from the

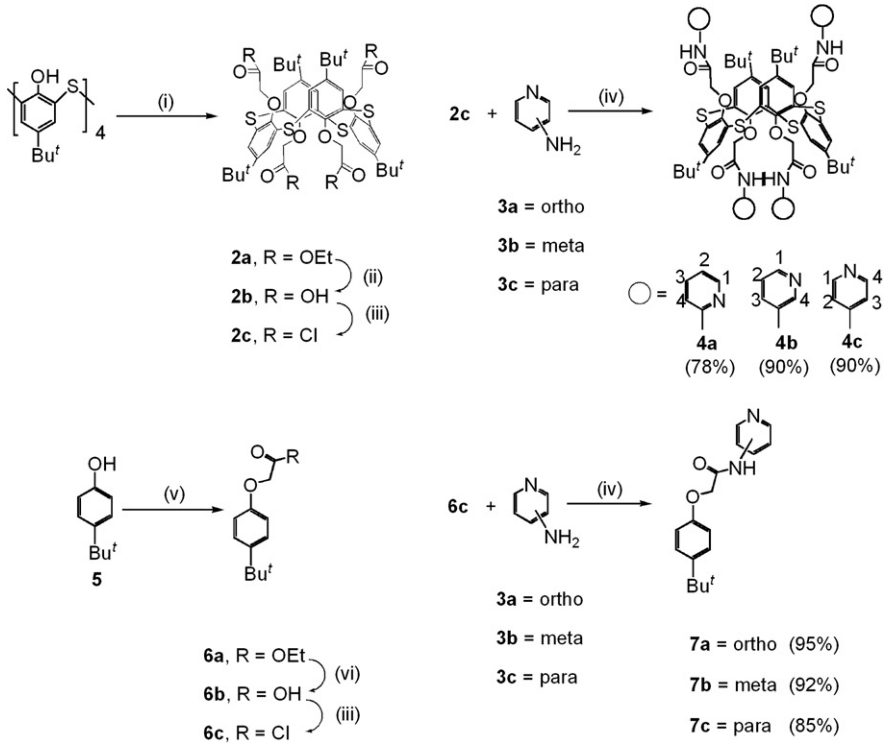

Scheme 1. (i) $BrCH_2COOCH_2CH_3$, Cs_2CO_3/acetone, reflux for 7 days; (ii) NaOH, EtOH/H_2O, reflux for 12 h; (iii) $SOCl_2/CH_2Cl_2$, reflux for 48 h; (iv) THF, reflux for 24 h; (v) $BrCH_2COOCH_2CH_3$, Na_2CO_3/acetone, reflux for 12 h; (vi) KOH, EtOH/H_2O, reflux for 12 h.

conformationally immobilized 1,3-alternate tetraacetate of known structure,[28] thus we speculated that it also adopted 1,3-alternate conformation.[25,29] The correlative reference compounds **7a–c** were also confirmed by the combination of ^{1}H NMR spectroscopy ESI-MS.

The final evidence for the 1,3-alternate conformation of thiacalixarene derivatives **4b** and **4c** was obtained by single-crystal X-ray crystallography as shown in the X-ray structures.

2.2. Solid-state self-assembly

Single crystals of **4b** and **4c** suitable for X-ray diffraction experiments were both obtained by slow evaporation of their dichloromethane/methanol mixed solution. As shown in the X-ray structures (Fig. 1), the thiacalixarenes are all in a 1,3-alternate conformation.

The thiacalixarene shape can be characterized by the values of the dihedral angles between the phenolic rings and the mean plane defined by the sulfur atoms, while the extent of perpendicularity differs from aromatic rings to aromatic rings in both of **4b** and **4c**. The consecutive four aromatic rings in **4b** make a dihedral angle of approximately 61°, 70°, 79°, and 73°. Whereas the dihedral angles defined are comparable to 67°, 70°, 82°, and 70°, respectively, found in the structure of **4c**. Therefore, the shape of thiacalixarene cores in **4b** and **4c** is extraordinarily close to each other, and both adopt a slightly pinched 1,3-alternate conformation, with no crystallographic symmetry.

In the solid state, compared with the shape of the thiacalixarene cores in **4b** and **4c**, their whole molecular structures show much more unsymmetrical, which could be ascribed to the spatial different outspread of the side chains possessing rotational flexibility. While the most significant conformational difference for **4b** and **4c** was the orientation of aminopyridyl side chain connected to the thiacalixarene skeleton, which result from the different position of connection of the amine group to the pyridyl group. For **4b**, it is possible for the sp^2 nitrogen donors in the *meta* position of the aminopyridyl groups to form intramolecular hydrogen bondings with the facing amide N–H of the adjacent aminopyridyl groups. As depicted in Figure 1, the amide N1 and N5 atoms in molecule at (*x*, *y*, *z*) acting as H-bonding donors, to pyridyl N4 and N8 atoms in the same molecule, respectively, form two intramolecular hydrogen bonds, thereinto, locating on two ends of the thiacalixarene core. In this conformation, all the amine NH protons orientate inwardly with respect to the framework and buried in the cavity of thiacalixarene, thus they could not form strong intermolecular hydrogen bond with adjacent ligands. In the case of 1,3-alternate thiacalix[4]arene derivative **4c**, the potential H-bonded amide N atoms N1/N3/N5/N7 do not form any intramolecular H-bonds with pyridyl N atoms due to the terminal position of the nitrogen atoms in the *para*-pyridyl moieties and are outwardly oriented with respect to the cavity. Such a conformation ensures that these amide N atoms in **4c** are available for intermolecular interactions with the pyridyl N atoms, a feature that helps to form infinite strong H-bonded Networks of **4c**.[11,15]

In designing these two structural isomers of receptors, we anticipated that their different conformations would give rise to different self-assembly properties, which was, in fact, the case. As can be readily seen from Figure 2, the tectons **4b** are interconnected via intermolecular C38–H38A$\cdots\pi$ interaction ($d_{H38A\cdots\pi}$=2.74 Å) between the O–CH_2 group in one of the lower rim substituent and one of the pyridyl subunit of neighboring thiacalix[4]arene and C35–H35B$\cdots$O2 interaction ($d_{O2\cdots H35B}$=2.72 Å) between the *tert*-butyl group and the carbonyl group, forming along the *b* axis a 1-D polymeric chain, in which thiacalixarene cavities are mutually oriented side-by-side.

Then two adjacent linear networks exhibit a staggered, antiparallel, up–down arrangement and are double stranded interwoven, leading thus to double stranded rectilineal networks (Fig. 3).[30] The driving force for the formation of this peculiar arrangement is related to the C62–H62A$\cdots$O6 interactions ($d_{O6\cdots H62A}$=2.43 Å) between the O–CH_2 groups belonging to one strand and carbonyl oxygen atoms of the other strand.

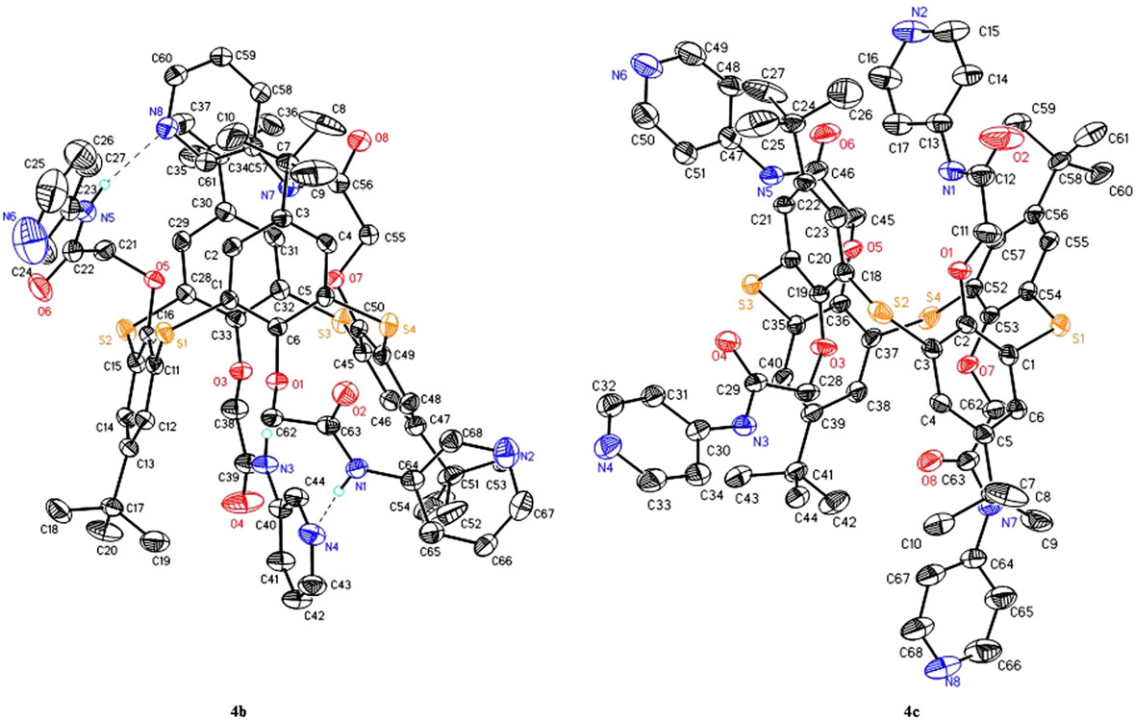

Figure 1. A perspective view of the different conformation of the aminopyridyl side chain on thiacalixarene skeleton in solid-state structures of **4b** (left) and **4c** (right) and its labeling scheme. Dotted lines indicate hydrogen bonds. The hydrogen atoms not involved in intramolecular H-bonding interaction and the solvent molecules are omitted for clarity.

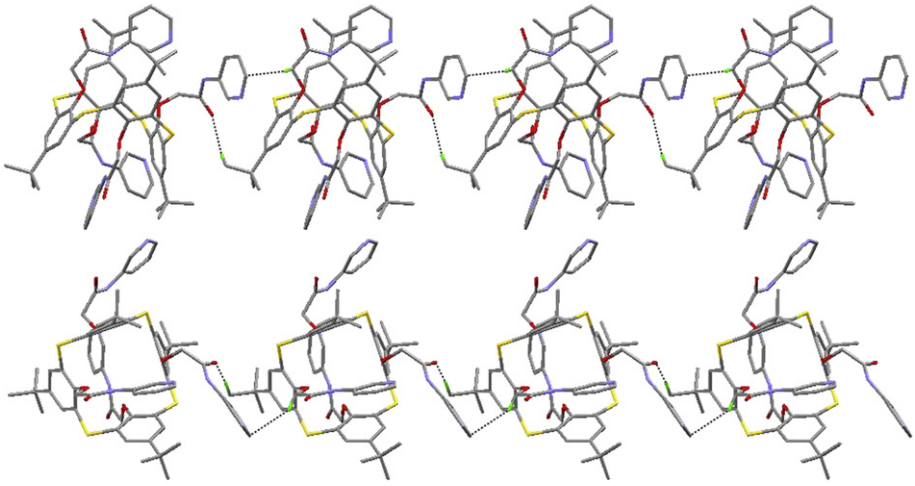

Figure 2. A portion of the X-ray structure showing the formation of single strand obtained by mutual C38–H38A···π and C35–H35B···O2 interactions of neighboring thiacalix[4]arene **4b**. Dotted lines evidence the intermolecular interactions. For clarity, H atoms not involved in intermolecular interactions, and solvent molecules and anions are not shown (up, view perpendicular to *a* axis; down, view perpendicular to *c* axis).

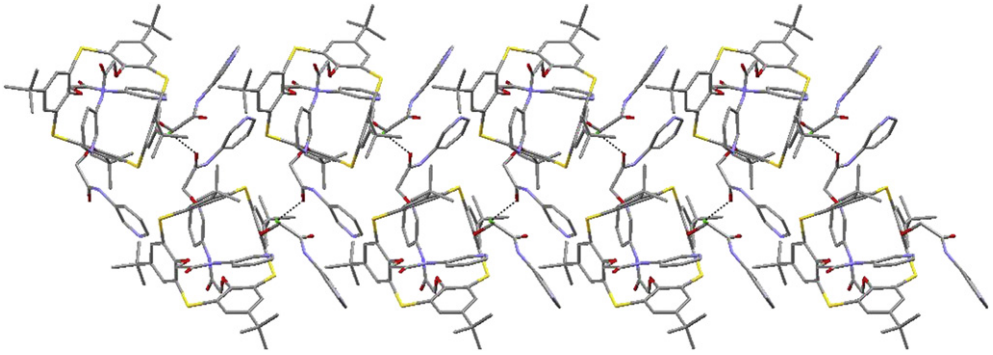

Figure 3. A portion of the X-ray structure showing the formation of double stranded interwoven rectilineal architecture resulting from the C62–H62A···O6 interactions between two adjacent single strands of thiacalix[4]arene **4b** (view perpendicular the *c* axis).

Solution of the diffraction data revealed an *endo* cavity asymmetric unit that comprises one thiacalix[4]arene and three disordered methanol molecules. Notably, methanol solvent molecules among the crystal lattice serve to link the individual double stranded rectilineal networks in the *c* axis and *ab* axis, respectively, which constructed the overall supramolecular assembly of the building blocks **4b**. However, the above solvent disorder features seemed to have a negligible effect, allowing for a precise determination of the interactions between the host and solvent molecules, as well as the driving force for the packing of the adjacent double stranded interwoven infinite linear networks.

In the overall crystal architecture of **4c**, the building blocks are held together by intermolecular H-bonds and solvent molecules play the role of the bridges between the individual thiacalixarenes. Thiacalix[4]arene neighbors are directly linked to one another via a strong intermolecular N7–H7···N4 H-bonds ($d_{N4\cdots H7}$=2.10 Å) between the amide N–H and the pyridyl nitrogens forming a 1-D polymeric chain along the *c* directions,[15] where the individual molecules of the macrocycle are in a side-by-side orientation (Fig. 4).[31] Two strips of the resulting 1-D networks are further connected by water molecules via a series of oppositely directed N2···H–O–H···O2 ($d_{N2\cdots H}$=2.20 Å and $d_{O2\cdots H}$=2.08 Å) bridges of hydrogen bonds to give a extended water-bridged double strands (Fig. 5).

Some solvent molecules such as methanol and dichloromethane are incorporated into the lattice during crystallization to fill the void space located among the individual water-bridged double strands. The overall crystal architecture is characterized by extended water-bridged double strand that propagate through the crystal along the *b* axis and *ac* axis, respectively, in which the adjacent double strands are indirectly interconnected via dichloromethane-mediated bridges.[32] However, the disorder of the

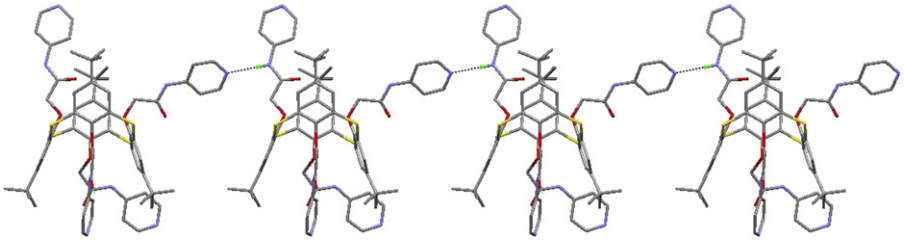

Figure 4. A portion of the X-ray structure showing the formation of single strand obtained by mutual N7–H7···N4 interactions of neighboring thiacalix[4]arene **4c** (view perpendicular the *a* axis).

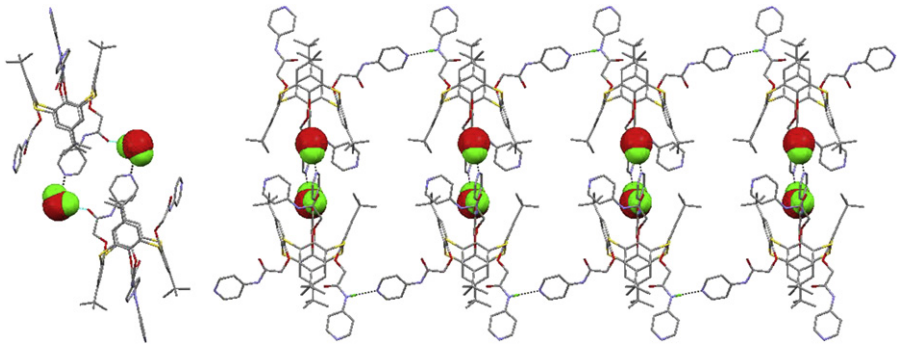

Figure 5. A portion of the X-ray structure showing the formation of the water-bridged double strand (left, view perpendicular to *c* axis; right, view perpendicular to *a* axis).

dichloromethane molecule prevents us from determining the type of the interactions between the dichloromethane and the building block **4c**, as well as giving an accurate account of the relative weak interaction fashion between the consecutive neighboring water-bridged double strands.

2.3. Complexation study

A first estimation of the ionophoric properties of ligands **4a–c** was accomplished by the picrate extraction method developed by Pedersen.[33] The results expressed as an association constants (K_a) are reported in Table 1, using the picrate extraction method reported by Lein and Cram,[34] which is more quantitative and allows a direct comparison of the ionophoric properties of compounds **4a–c** with each other, the values of association constants (K_a) are listed in Table 1. A comparison with *p-tert*-butylthiacalix[4]arene **1** was also provided.

Two-phase solvent extraction experiments reveal that the introduction of the aminopyridine groups into the lower rim of the thiacalixarene skeleton fixed in the 1,3-alternate conformation could enhance its selectivity and affinity for Ag^+ with different efficiencies depending on the side chain. It is clear from Table 1 that when the terminal group on the side chain is *ortho*-pyridyl, the K_a value for silver picrate is only twice higher than that of the parent thiacalix[4]arene **1** (10.62×10^6 and 5.09×10^6, respectively). However, when the terminal group is *para*-pyridyl, there is almost a fivefold increase in K_a value for silver picrate. The highest increase in extraction of Ag^+ is observed when the terminal group is *meta*-pyridyl, whose K_a value for silver picrate is nearly 19 times higher than that of ionophore **1**. This data indicate that the efficiency of ligands **4a–c** in the complexation of silver ion should be sensitive mainly to the position of nitrogen in the pyridine rings.

In order to gain insight into the extraction mechanism, ^{1}H NMR titration experiments were carried out. Titrations of ligands **4a–c** with silver perchlorate in $CDCl_3$/DMSO-d_6=1:1 (v/v) at 298 K did not cause the appearance of new signals, but led to the distinct change in the chemical shifts to indicate fast metal exchange between complexed and uncomplexed species on the NMR time scale at room temperature. During the titration of **4b**, distinct change in the chemical shift was observed in the region of the aminopyridyl group. Figure 6 shows the change in the chemical shift of the aminopyridyl protons ($\Delta\delta$) plotted against the amount of silver perchlorate added. The $\Delta\delta$ value increased in proportion to the amount of the perchlorate added and became constant after the addition of 1.0 mol equiv of the perchlorate, indicating that the stoichiometry of the complex is 1:1 in the solution. Similar phenomena also occurred in the case of **4a** and **4c**. The 1:1 stoichiometry of Ag^+ complex of the ligands **4a–c** was also confirmed by ESI-MS. After 24 h precomplexation between ligands **4a–c** with 4 equiv of $AgClO_4$ in $CHCl_3$/DMSO (1:1), respectively, all of their electrospray mass spectrometry showed two most intense peaks at m/z 1363.3 and 1365.3 corresponding to the [ligand+$^{107}Ag^+$] and [ligand+$^{109}Ag^+$] ions, respectively.

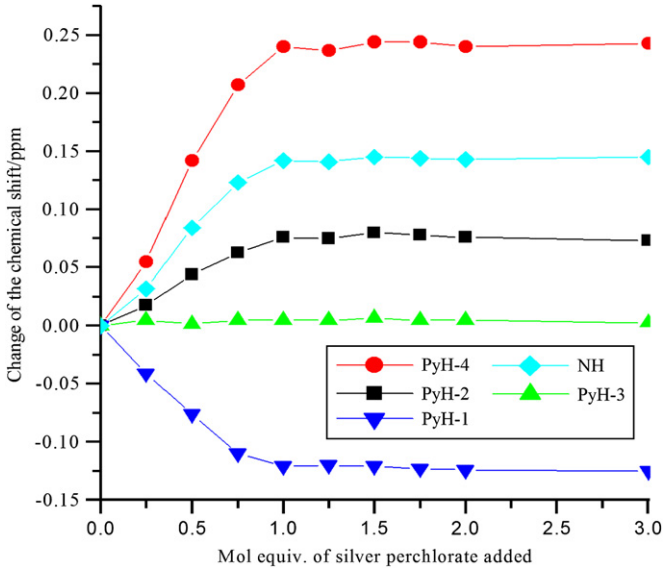

Figure 6. ^{1}H NMR titration of **4b** with $AgClO_4$ in $CDCl_3$/DMSO-d_6=1:1 (v/v).

Although more or less the same situations were found after the addition of silver perchlorate to ligands **4a–c**, there are some differences in their Ag^+ binding sites. Comparison of ^{1}H NMR chemical shifts between free and Ag^+ complexed ligands can investigate their Ag^+ binding sites and precisely explain the influence of the structure of the aminopyridyl group on the complexation ability, which is shown in Table 2. Since the present studies have been performed in neutral media, it would be anticipated that such

Table 1
Association constants ($K_a\times10^{-5}$) for complexes of metal picrates with ionophores in $CHCl_3$

	Li^+	Na^+	K^+	Cs^+	Co^{2+}	Ni^{2+}	Cu^{2+}	Zn^{2+}	Ag^+
1	24.2	12.6	9.1	8.7	5.8	—	16.2	5.4	50.9
4a	9.34	13.2	14.8	2.24	—	—	5.34	2.47	106.2
4b	17.5	—	—	—	23.3	9.16	57.8	—	937.3
4c	1.13	—	3.80	1.11	13.1	1.29	4.26	—	270.8

'—' Denotes the value of K_a less than 10^5.

Table 2
Comparison of ^{1}H NMR chemical shifts (δ) between free and Ag^+ complexed ligands in the ^{1}H NMR titration experiments

Host	Thiacalixarene		Side chain					
	t-BuH	ArH	OCH_2	PyH-1	PyH-2	PyH-3	PyH-4	NH
4a	0.672	7.594	4.992	8.175	6.959	7.618	8.204	8.841
4a+Ag^+	0.706	7.592	4.949	8.161	7.004	7.654	8.221	8.999
$\Delta\delta$	0.034	−0.02	−0.043	−0.014	0.045	0.036	0.017	0.158
4b	0.708	7.308	4.686	8.451	7.425	8.424	8.319	9.191
4b+Ag^+	0.758	7.351	4.592	8.330	7.501	8.429	8.559	9.333
$\Delta\delta$	0.05	0.043	−0.094	−0.121	0.076	0.005	0.24	0.142
4c	0.863	7.492	4.653	8.457	7.507	7.507	8.457	8.757
4c+Ag^+	0.937	7.525	4.629	8.503	7.665	7.665	8.503	9.221
$\Delta\delta$	0.074	0.033	−0.024	0.046	0.158	0.158	0.046	0.464

compounds should behave as binding ligands through the aminopyridyl oxygen and sp^2 nitrogen atoms rather than amide nitrogen atoms.[35] The largest downfield shifts of ligands **4a** and **4c** were measured for the amido protons (NH), this could be indicative of a form of coordination as simple as a two-point ligation, which occurs with the primary oxygen donors of the amido groups and form a sandwich-like complex with Ag^+. In the case of **4a**, it is unexpected that the sp^2 nitrogen atom in the *ortho* position whose lone-pair electron oriented toward the cavity center did not play considerable role in complexation as reflected by the small $\Delta\delta$ values of PyH=−0.01 to +0.05 ppm. The unusual observation may result from that amide unit, which locates so close to the sp^2 nitrogen atom in the *ortho* position that would disturb its binding to Ag^+. In the 1,3-alternate-**4c**·Ag^+ system, it is impossible for the pyridyl nitrogen atoms to interact with Ag^+ due to the terminal position of the nitrogen atom in the *para*-pyridyl moiety, which can be affirmed by the crystal structures of **4c** (Fig. 1). Thus, one can consider that the downfield shift of the *para*-pyridyl protons (+0.05 and +0.16 ppm, respectively) is due to the inductive effect arising from the interaction between the amido oxygen donors and Ag^+. On the other hand, it is well known that the electron-withdrawing effect of the sp^2 nitrogen atom toward the amide group in the *ortho* position is stronger than that in the *para* position, so the basicity of the amide oxygen atom in ligand **4a** would be weaker than that in ligand **4c**, thereby it provides a more favorable ligating site for binding, which is shown by the smaller downfield shift of the NH proton (0.16 vs 0.46 ppm). This is in agreement with the extraction results that the association constant (K_a) of **4a**·Ag^+ complex is lower than that of **4c**·Ag^+ complex.

With ligand **4b** a quite different situation was found upon complexation with Ag^+. As indicated in the crystal structures of **4b** (Fig. 1), the *meta* position of the nitrogen atoms in the aminopyridyl groups that makes just half of the sp^2 nitrogen donors could form hydrogen bondings with the facing amide N–H of the adjacent aminopyridyl groups, only if two of the four side chains show marked distortion. So it is presumable that the weaker hydrogen bonding system of **4b** might be broken and the sp^2 nitrogen atom would complex Ag^+ when the metal cation approach the cavity of the ligand. As expected, the most marked downfield shifts are experienced by the amido proton (0.14 ppm) followed by PyH-4 proton *ortho* to N of pyridyl (0.24 ppm), thus it is can be inferred that the ligand **4b** binds the silver ion mainly by the pyridyl nitrogen atoms with the assistance of carbonyl oxygen donors. We consider, therefore, that the best Ag^+ extraction ability of **4b** among the three ligands is attributed to preferred interaction between the soft nitrogen donor atoms and the soft Ag^+ ion.[7]

To determine whether Ag^+ binding is an intrinsic property of ligands **4a–c** or a general property of hydrophobic amidopyridyl units, 4-*tert*-butyl-(pyridyl-carbamoyl-methoxy)-benzenes **7a–c** (Fig. 1) were tested in the two-phase solvent extraction experiments. Compounds **7a–c** are the respective monomeric analogs of thiacalixarenes **4a–c**, bearing aminopyridyl functions that could bind Ag^+, but lacking the thiacalixarene's macrocycle. The standard extraction assay even in the presence of high excess of **7a–c** showed that no Ag^+ was extracted into the $CHCl_3$ solution. In addition, spectroscopy indicated no Ag^+ binding by **7a–c** in $CDCl_3$/DMSO-d_6 (1:1). These controls with 4-*tert*-butyl-(pyridyl-carbamoyl-methoxy)-benzenes **7a–c** support the hypothesis that the 1,3-alternate thiacalixarene's core is critical for the Ag^+ binding properties of **4a–c**.

3. Conclusions

Tetraaminopyridyl-thiacalix[4]arene derivatives (**4a–c**) in the 1,3-alternate conformation were synthesized. It was found that their self-assembly behavior strongly depended on the structure of aminopyridyl pendent arms. Two crystal structures demonstrated that tetra(*meta*-aminopyridyl)-TCA motif is capable of forming a double stranded rectilineal networks, where the thiacalixarene is preorganized in a side-by-side arrangement, by contrast, tetra-(*para*-aminopyridyl)-TCA self-assembles via hydrogen bondings to generate solid-state structure with water-bridged double strand, which is the first example of encapsulation of water molecules within an organized network of thiacalixarene derivative. Further development of this self-assembly motif in the field of crystal engineering to design functional materials is possible since thiacalixarenes offer the potential of controlling the self-assembly pattern by the nature of the substituents on the thiacalixarene core.

On the other hand, their complexation study indicated that all the ligands **4a–c** show Ag^+ ion selectivity over other metal cations and the binding efficiency is influenced by the structures of aminopyridyl pendent arms. In the case of *meta*-aminopyridyl compound **4b**, the sp^2 nitrogen and carbonyl oxygen donors in amidopyridyl unit possess the most advantaged steric arrangement, thus it shows the best extraction capacity. Therefore, in the design of the tetraaminopyridyl-thiacalix[4]arene derivatives to optimize the metal ion affinity, amidopyridyl group of the *meta*-isomer should be mostly considered.

4. Experimental

4.1. General

Melting points are uncorrected. The ^{1}H NMR and ^{13}C NMR spectra were recorded at 298 K in $CDCl_3$ at 300 MHz and 75 MHz, respectively, on a Varian Mercury-VX300 spectrometer. The chemical shifts were recorded in parts per million (ppm) with TMS as the internal reference. ESI mass spectra were determined using a Finnigan LCQ Advantage mass spectrometer. Elemental analyses were performed with a Thermo Quest Flash EA1112 apparatus. UV–vis spectra were recorded on a Shimadzu UV-1601 spectrophotometer. X-ray data were recorded using a Bruker SMART CCD single-crystal diffractometer. compound *p*-*tert*-butylthiacalixarene was synthesized by the method described by Kumagai and

co-workers.[21] 1,3-Alternate *p-tert*-butylthiacalixarene tetraacetate was synthesized according to the literature procedure,[24] the corresponding carboxylic acid **2b** was synthesized as described in the literature.[25]

4.2. General procedure for the synthesis of 1,3-alternate thiacalix[4]arene tetraaminopyridyl derivatives (compounds 4a–c)

A mixture of acid **2b** (0.23 g, 0.24 mmol) and thionyl chloride (0.8 mL, 11.2 mmol) in dichloromethane (10 mL) was reflux for 48 h. Removal of the solvent and residual thionyl chloride under reduce pressure furnished the acid chloride **2c** as an off-white solid. The crude product **2c** was cooled to room temperature and dissolved in THF (15 mL), and then aminopyridine (0.23 g, 2.45 mmol) was added. The stirred mixture was refluxed under N_2 atmosphere, then approximate half of the solvent was distilled off, and the residue was treated with 10 mL of distilled water; after filtration, the precipitate was washed with distilled water (3×10 mL) to give a yellow to dark red precipitate and the mixture of products was then separated by column chromatography (silica gel) to give the thiacalix[4]arene tetraaminopyridyl derivatives.

4.2.1. 5,11,17,23-Tetra-tert-butyl-25,26,27,28-tetrakis[(2-pyridyl)-carbamoyl-methoxy]-2,8,14,20-tetrathiacalix[4]arene, ***4a***

Obtained as a white solid. Yield: 78%, mp>270 °C. ^{1}H NMR (300 MHz, $CDCl_3$): δ 0.74 (s, 36H, C(CH_3)$_3$), 5.09 (s, 8H, ArOCH_2), 7.01 (dd, J_1=7.2 Hz, J_2=5.1 Hz, 4H, Py*H*), 7.63–7.66 (m, 12H, Ar*H*+Py*H*), 8.26 (d, J=5.1 Hz, 4H, Py*H*), 8.28 (d, J=9 Hz, 4H, Py*H*), 9.01 (br s, 4H, N*H*). ^{13}C NMR (75 MHz, $CDCl_3$): 30.5, 34.1, 68.8, 114.7, 120.1, 126.4, 130.0, 137.8, 148.0, 150.9, 155.5, 168.1. MS ESI$^+$ *m*/*z*: 1257.4 [MH^+] (100%). EA calcd for $C_{68}H_{72}N_8O_8S_4$: C, 64.94; H, 5.77; N, 8.91; S, 10.20%. Found: C, 64.79; H, 5.72; N, 8.86; S, 10.16%.

4.2.2. 5,11,17,23-Tetra-tert-butyl-25,26,27,28-tetrakis[(3-pyridyl)-carbamoyl-methoxy]-2,8,14,20-tetrathiacalix[4]arene, ***4b***

Obtained as a white solid. Yield: 90%, mp>280 °C. ^{1}H NMR (300 MHz, $CDCl_3$): δ 0.70 (s, 36H, C(CH_3)$_3$), 4.71 (s, 8H, ArOCH_2), 7.30 (s, 8H, Ar*H*), 7.39 (dd, J_1=7.5 Hz, J_2=4.8 Hz, 4H, Py*H*), 8.28 (s, 4H, Py*H*), 8.42 (d, J=4.8 Hz, 4H, Py*H*), 8.55 (d, J=8.1 Hz, 4H, Py*H*), 9.25 (br s, 4H, N*H*). ^{13}C NMR (75 MHz, $CDCl_3$): 30.6, 34.3, 69.3, 124.5, 127.5, 129.0, 130.1, 136.6, 141.1, 144.8, 148.6, 166.0. MS ESI$^+$ *m*/*z*: 1257.5 [MH^+] (100%). EA calcd for $C_{68}H_{72}N_8O_8S_4$: C, 64.94; H, 5.77; N, 8.91; S, 10.20%. Found: C, 64.67; H, 5.80; N, 8.90; S, 10.10%.

4.2.3. 5,11,17,23-Tetra-tert-butyl-25,26,27,28-tetrakis[(4-pyridyl)-carbamoyl-methoxy]-2,8,14,20-tetrathiacalix[4]arene, ***4c***

Obtained as a white solid. Yield: 90%, mp>250 °C. ^{1}H NMR (300 MHz, $CDCl_3$): δ 0.74 (s, 36H, C(CH_3)$_3$), 4.86 (s, 8H, ArOCH_2), 7.47–7.50 (m, 16H, Py*H* +Ar*H*), 8.57 (d, J=6.0 Hz, 8H, Py*H*), 8.59 (s, 4H, N*H*). ^{13}C NMR (75 MHz, $CDCl_3$): 30.6, 34.5, 70.7, 113.7, 127.2, 130.9, 144.2, 149.8, 151.3, 156.2, 166.7. MS ESI$^+$ *m*/*z*: 1257.4 [MH^+] (100%). EA calcd for $C_{68}H_{72}N_8O_8S_4$: C, 64.94; H, 5.77; N, 8.91; S, 10.20%. Found: C, 64.79; H, 5.81; N, 8.86; S, 10.13%.

4.3. General procedure for the synthesis of ethyl *p-tert*-butylphenoxyacetate 6a

To a mixture of *p*-*tert*-butyl-phenol (1.50 g, 10 mmol) and Na_2CO_3 (1.06 g, 10 mmol) in dry acetone (100 mL) was added ethyl bromoacetate (2.00 g, 12 mmol). The mixture was refluxed for 12 h, cooled at room temperature, and concentrated under reduced pressure. The residue was dissolved in $CHCl_3$ and washed with 1 mol/L HCl. The organic layer was separated, washed with brine (2×15 mL), and dried over anhydrous $MgSO_4$. After filtration, the solvent was evaporated to dryness to obtain the pure product as a yellow oil in a 99% yield. ^{1}H NMR (300 MHz, $CDCl_3$): δ 1.29 (s, 9H, C(CH_3)$_3$), 1.33 (t, 3H, J=6.6 Hz, CH_2CH_3), 4.27 (q, 2H, J=7.2 Hz, CH_2CH_3), 4.60 (s, 2H, OCH_2), 6.85 (d, 2H, J=8.7 Hz, Ar*H*), 7.31 (d, 2H, J=8.7 Hz, Ar*H*).

4.4. General procedure for the synthesis of (4-*tert*-butyl-2, 6-dimethyl)phenoxyacetic acid 6b

A mixture of **6a** (2.36 g, 10 mmol) and potassium hydroxide (1.16 g, 20.7 mmol) in 90 mL of ethanol/water (2:l, v/v) was heated at 100 °C for 12 h, the solvent was evaporated under reduced pressure, and 50 mL of HCl (1 mol/L) and 50 mL of $CHCl_3$ were added. The organic phase was washed with purified water (3×50 mL), dried over anhydrous $MgSO_4$, and then all volatiles were removed at reduced pressure to afford a yellow oil in a 90% yield. ^{1}H NMR (300 MHz, $CDCl_3$): δ 1.30 (s, 9H, C(CH_3)$_3$), 4.67 (s, 2H, OCH_2CO), 6.87 (d, 2H, J=4.5 Hz, ArH), 7.33 (d, 2H, J=4.5 Hz, ArH).

4.5. General procedure for the synthesis of reference compounds (compounds 7a–c)

The reaction step was used as described for the preparation of **4a**–**c**. After the reaction finished, the solvent was removed under reduced pressure and the residue was washed with purified water. Then all volatiles were removed at reduced pressure to afford the reference compounds.

4.5.1. 4-tert-Butyl-[(2-pyridyl)-carbamoyl-methoxy]benzene, ***7a***

Obtained as a yellow oil. Yield: 95%. ^{1}H NMR (300 MHz, $CDCl_3$): δ 1.32 (s, 9H, C(CH_3)$_3$), 4.62 (s, 2H, ArOCH_2), 6.94 (d, 2H, J=9 Hz, Ar*H*), 7.08–7.12 (m, 1H, Py*H*), 7.35 (d, 2H, J=9 Hz, Ar*H*), 7.74–7.79 (m, 1H, Py*H*), 8.30–8.35 (m, 2H, Py*H*), 9.15 (br s, 1H, N*H*). MS ESI$^+$ *m*/*z*: 284.2 [M^+] (100%).

4.5.2. 4-tert-Butyl-[(3-pyridyl)-carbamoyl-methoxy]benzene, ***7b***

Obtained as a yellow oil. Yield: 92%. ^{1}H NMR (300 MHz, $CDCl_3$): δ 1.32 (s, 9H, C(CH_3)$_3$), 4.64 (s, 2H, ArOCH_2), 6.94 (d, 2H, J=8.7 Hz, Ar*H*), 7.35–7.39 (m, 3H, Ar*H*+Py*H*), 8.27 (d, 1H, J=8.7 Hz, Py*H*), 8.41 (d, 1H, J=4.5 Hz, Py*H*), 8.51 (s, 1H, Py*H*), 8.70 (s, 1H, N*H*). MS ESI$^+$ *m*/*z*: 284.3 [M^+] (100%).

4.5.3. 4-tert-Butyl-[(4-pyridyl)-carbamoyl-methoxy]benzene, ***7c***

Obtained as a yellow oil. Yield: 85%. ^{1}H NMR (300 MHz, $CDCl_3$): δ 1.31 (s, 9H, C(CH_3)$_3$), 4.65 (s, 2H, ArOCH_2), 6.92 (d, 2H, J=9 Hz, Ar*H*), 7.39 (d, 2H, J=7 Hz, Ar*H*), 7.51 (d, 2H, J=6 Hz, Py*H*), 8.61 (d, 2H, J=6 Hz, Py*H*), 8.76 (s, 1H, N*H*). MS ESI$^+$ *m*/*z*: 284.1 [M^+] (100%).

4.6. X-ray structural determination of 4b

$C_{68}H_{72}N_8O_8S_4\cdot 3CH_3OH$, M=1321.66, monoclinic, a=37.7549(16) Å, b=12.7784(6) Å, c=30.4133(13) Å, α=90°, β=108.6850(10)°, γ=90°, V=3154.5(4) Å^3, space group=$C2/c$, Z=8, D_c=1.263 Mg/m^3, μ=0.199 mm^{-1}. Intensity data were collected up to θ=25.50° by using 2θ scanning mode with graphite filtered Mo Kα radiation (λ=0.71073) on a 0.30×0.20×0.20 mm^3 crystal at 294(2) K. A total of 67,987 reflections were measured, 12,914 were independent, and of which 8339 [I>2(I)] were considered observed. The structure was solved by direct methods using SHELXS97[36]and refined by Full-matrix least-squares on F^2 using SHELXL97.[37] All the non-hydrogen atoms were located directly by successive Fourier calculations and were refined anisotropically. Hydrogen atoms were placed in geometrically calculated positions by using a riding model. No absorption correction was applied. Final R indices [I>2σ(I)] $R1$=0.0642, $wR2$=0.1740, and R indices (all data) $R1$=0.1029, $wR2$=0.1928 was found for 12,914 independent

reflections, 1 restraints, and 876 parameters. The GOF value is 1.003. Crystallographic data (excluding structural factors) for the structures in this paper have been deposited with the Cambridge Crystallographic Data Centre as supplementary publication no. CCDC 674705. Copies of the data can be obtained, free of charge, on application to CCDC, 12 Union Road, Cambridge CB2 1EZ, UK (fax: +44 (0)1223 336033 or e-mail: deposit@ccdc.cam.ac.uk).

4.7. X-ray structural determination of 4c

$C_{68}H_{72}N_8O_8S_4 \cdot CH_2Cl_2 \cdot 2CH_3OH \cdot 2H_2O$, M=1424.54, monoclinic, a=13.7252(16) Å, b=35.497(4) Å, c=15.3054(18) Å, α=90°, β=93.524(2)°, γ=90°, V=7442.8(15) Å^3, space group=$P2(1)/n$, Z=4, D_c=1.271 Mg/m^3, μ=0.262 mm^{-1}. Intensity data were collected up to θ=22.63° by using 2θ scanning mode with graphite filtered Mo Kα radiation (λ=0.71073) on a 0.30×0.10×0.10 mm^3 crystal at 295(2) K. A total of 77,457 reflections were measured, 14,584 were independent, and of which 7958 [$I>2(I)$] were considered observed. Final R indices [$I>2\sigma(I)$] $R1$=0.0771, $wR2$=0.2084, and R indices (all data) $R1$=0.1289, $wR2$=0.2348 was found for 14,584 independent reflections, 36 restraints, and 919 parameters. The GOF value is 0.994. The apparent high R values are possibly due to the disorder found in one of the *tert*-butyl groups and the solvent molecules. The structure was solved by direct methods using SHELXS97[36] and refined by Full-matrix least-squares on F^2 using SHELXL97.[37] All the non-hydrogen atoms were located directly by successive Fourier calculations and were refined anisotropically except for an oxygen atom of one lattice solvent molecule of methanol. Hydrogen atoms except for that of the disordered lattice solvent molecule were placed in geometrically calculated positions by using a riding model. No absorption correction was applied. Crystallographic data (excluding structural factors) for the structures in this paper have been deposited with the Cambridge Crystallographic Data Centre as supplementary publication no. CCDC 674706. Copies of the data can be obtained, free of charge, on application to CCDC, 12 Union Road, Cambridge CB2 1EZ, UK (fax: +44 (0)1223 336033 or e-mail: deposit@ccdc.cam.ac.uk).

Acknowledgements

We are grateful to the National Natural Science Foundation of China (20772092) and the Hubei Province Natural Science Fund for Distinguished Young Scholars (2007ABB021) for financial support.

References and notes

1. (a) Gutsche, C. D. *Calixarenes*; Stoddart, J. F., Ed.; Monographs in Supramolecular Chemistry; The Royal Society of Chemistry: Cambridge, 1989; (b) Ikeda, A.; Shinkai, S. *Chem. Rev.* **1997**, *97*, 1713; (c) *Calixarenes in Action*; Mandolini, L., Ungaro, R., Eds.; Imperial College Press: London, 2000; (d) *Calixarenes 2001*; Asfari, Z., Böhmer, V., Harrowfield, J. M., Vicens, J., Eds.; Kluwer Academic: Dordrecht, 2001.
2. Gutsche, C. D. *Calixarenes Revisited*; Stoddart, J. F., Ed.; Monographs in Supramolecular Chemistry; The Royal Society of Chemistry: Cambridge, 1998.
3. (a) *Cation Binding by Macrocycles*; Inoue, Y., Gokel, G. W., Eds.; Marcel Dekker: New York, NY, 1990; (b) Gokel, G. W. *Crown Ethers and Cryptands*; The Royal Society of Chemistry: London, England, 1991.
4. (a) Wenz, G. *Angew. Chem., Int. Ed. Engl.* **1994**, *33*, 803; (b) Szejtli, J. *Cyclodextrins and their Inclusion Complexes*; Akademjai Kiado: Budapest, 1982; (c) *Comprehensive Supramolecular Chemistry*; Szejtli, J., Osa, T., Eds.; Pergamon: Elsevier, Oxford, 1996; Vol. 3, (Cyclodextrins).
5. Casnati, A.; Ungaro, R. Calixarenes in Spherical Metal Ion Recognition. In *Calixarenes in Action*; Mandolini, L., Ungaro, R., Eds.; Imperial College Press: London, 2000; Chapter 4.
6. (a) Ikeda, A.; Shinkai, S. *J. Am. Chem. Soc.* **1994**, *116*, 3102; (b) Ikeda, T.; Tsudera, T.; Shinkai, S. *J. Org. Chem.* **1997**, *62*, 3568; (c) Tsudera, T.; Ikeda, A.; Shinkai, S. *Tetrahedron* **1997**, *53*, 13609; (d) Chen, L.; Zeng, X.; He, X.; Zhang, Z. Z.; Fresenius, J. *Anal. Chem.* **2000**, *367*, 535; (e) Kimura, K.; Yayima, S.; Tatsumu, K.; Yokoyama, M.; Oue, M. *Anal. Chem.* **2000**, *72*, 5290; (f) Zeng, X.; Sun, H.; Chen, L.; Leng, X.; Xu, F.; Li, Q.; He, X.; Zhang, W.; Zhang, Z. Z. *Org. Biomol. Chem.* **2003**, 1073; (g) Demirel, A.; Dogan, A.; Akkus, G.; Yilmaz, M.; Kilic, E. *Electroanalysis* **2006**, *18*, 1019.
7. Csokai, V.; Grün, A.; Balázs, B.; Simon, A.; Tóthb, G.; Bitter, I. *Tetrahedron* **2006**, *62*, 10215.
8. (a) Bozkurt, S.; Karakucuk, A.; Sirit, A.; Yilmaz, M. *Tetrahedron* **2005**, *61*, 10443; (b) Fontàs, C.; Anticó, E.; Vocanson, F.; Lamartine, R.; Seta, P. *Sep. Purif. Technol.* **2007**, *54*, 322.
9. Simard, M.; Su, D.; Wuest, J. D. *J. Am. Chem. Soc.* **1991**, *113*, 4696.
10. (a) Burrows, A. D. *Struct. Bond.* **2004**, *108*, 55; (b) Metrangolo, P.; Resnati, G. *Chem.—Eur. J.* **2001**, *7*, 2511; (c) Casnati, A.; Liantonio, R.; Metrangolo, P.; Resnati, G.; Ungaro, R.; Ugozzoli, F. *Angew. Chem., Int. Ed.* **2006**, *45*, 1915.
11. Hosseini, M. W. *Acc. Chem. Res.* **2005**, *38*, 313.
12. Baldini, L.; Sansone, F.; Massera, C.; Casnati, A.; Ugozzoli, F.; Ungaro, R. *Inorg. Chim. Acta* **2007**, *360*, 970.
13. Sansone, F.; Segura, M.; Ungaro, R. Calixarenes in Bioorganic and Biomimetic Chemistry. In *Calixarenes 2001*; Asfari, Z., Böhmer, V., Harrowfield, J., Vicens, J., Eds.; Kluwer Academic: Dordrecht, The Netherlands, 2001; Chapter 27.
14. (a) Prins, L. J.; Reinhoudt, D. N.; Timmerman, P. *Angew. Chem., Int. Ed.* **2001**, *40*, 2383; (b) Casnati, A.; Sansone, F.; Ungaro, R. *Acc. Chem. Res.* **2003**, *36*, 246.
15. Seganish, J. L.; Santacroce, P. V.; Salimian, K. J.; Fettinger, J. C.; Zavalij, P.; Davis, J. T. *Angew. Chem., Int. Ed.* **2006**, *45*, 3334.
16. Cho, Y. L.; Rudkevich, D. M.; Shivanyuk, A.; Rissanen, K.; Rebek, J. *Chem.—Eur. J.* **2000**, *6*, 3788.
17. Rebek, J. *Chem. Commun.* **2000**, 637.
18. Kasyan, O.; Kalchenko, V.; Bolteb, M.; Böhmer, V. *Chem. Commun.* **2006**, 1932.
19. (a) Hosseini, M. W. *CrystEngComm* **2004**, *6*, 318; (b) Bosch, E. *CrystEngComm* **2007**, *9*, 191.
20. Pansanel, J.; Jouaiti, A.; Ferlay, S.; Hosseini, M. W.; Planeix, J. M.; Kyritsakas, N. *New J. Chem.* **2006**, *30*, 71.
21. Kumagai, H.; Hasegawa, M.; Miyanari, S.; Sugawa, Y.; Sato, Y.; Hori, T.; Ueda, S.; Kamiyama, H.; Miyano, S. *Tetrahedron Lett.* **1997**, *38*, 3971.
22. (a) Iki, N.; Miyano, S. *J. Inclusion Phenom. Macrocycl. Chem.* **2002**, *4*, 99; (b) Lhotak, P. *Eur. J. Org. Chem.* **2004**, 1675.
23. Morohashi, N.; Narumi, F.; Iki, N.; Hattori, T.; Miyano, S. *Chem. Rev.* **2006**, *106*, 5291.
24. (a) Akdas, H.; Mislin, G.; Graf, E.; Hosseini, M. W.; Cian, A. D.; Fischer, J. *Tetrahedron* **1999**, *40*, 2113; (b) Lhoták, P.; Stastny, V.; Zlatusková, P.; Stibor, I.; Michlová, V.; Tkadlecová, M.; Havlicek, J.; Sykora, J. *Collect. Czech. Chem. Commun.* **2000**, *65*, 757.
25. Zlatušková, P.; Stibor, I.; Tkadlecová, M.; Lhoták, P. *Tetrahedron* **2004**, *60*, 11383.
26. (a) Lamartine, R.; Bavoux, C.; Vocanson, F.; Martin, A.; Senlisb, G.; Perrinb, M. *Tetrahedron Lett.* **2001**, *42*, 1021.
27. (a) Iki, N.; Narumi, F.; Fujimoto, T.; Morohashi, N.; Miyano, S. *J. Chem. Soc., Perkin Trans. 2* **1998**, *2*, 2745; (b) Iwamoto, K.; Araki, K.; Shinkai, S. *Tetrahedron* **1991**, *47*, 4325; (c) Aruand-Neu, F.; Collins, E. M.; Deasy, M.; Ferguson, G.; Harris, W. J.; Kaituer, B.; Lough, A. J.; Mckervey, M. A.; Marques, E.; Ruhl, B. L.; Weill, M. J. S.; Seward, E. M. *J. Am. Chem. Soc.* **1989**, *111*, 8681; (d) Yamato, T.; Zhang, F. L.; Kumamaru, K.; Yamamoto, K. *J. Inclusion Phenom. Macrocycl. Chem.* **2002**, *42*, 51.
28. van Leeuwen, F. W. B.; Beijleveld, H.; Koojiman, H.; Spek, A. L.; Verboom, W.; Reinhoudt, D. N. *Tetrahedron Lett.* **2002**, *43*, 9675.
29. (a) Dudic, M.; Lhoták, P.; Stibor, I.; Dvořáková, H.; Lang, K. *Tetrahedron* **2002**, *58*, 5475; (b) Šťastný, V.; Stibor, I.; Dvořáková, H.; Lhoták, P. *Tetrahedron* **2004**, *60*, 3383.
30. Hosseini, M. W. *Chem. Commun.* **2005**, 5825.
31. Sýkora, J.; Himl, M.; Stibor, I.; Císařová, I.; Lhoták, P. *Tetrahedron* **2007**, *63*, 2244.
32. Gil-Ramírez, G.; Benet-Buchholz, J.; Escudero-Adán, E. C.; Ballester, P. *J. Am. Chem. Soc.* **2007**, *129*, 3820.
33. Pedersen, C. J. *Fedn. Proc.* **1968**, *27*, 1305.
34. (a) Lein, G. M.; Cram, D. J. *J. Am. Chem. Soc.* **1985**, *107*, 448; (b) Helgeson, R. C.; Weisman, G. R.; Toner, J. L.; Tamowski, T. L.; Chau, L.; Mayer, J. M.; Cram, D. J. *J. Am. Chem. Soc.* **1979**, *101*, 4928.
35. (a) Clement, O.; Rapko, B. M.; Hay, B. P. *Coord. Chem. Rev.* **1998**, *170*, 203; (b) Pessoa, J. C.; Correia, I.; Kiss, T.; Jakusch, T.; Castro, M. M. C. A.; Geraldes, C. F. G. C. *J. Chem. Soc., Dalton Trans.* **2002**, 4440; (c) Singh, N.; Kumar, M.; Hundal, G. *Tetrahedron* **2004**, *60*, 5393; (d) Bhalla, V.; Kumar, M.; Katagiri, H.; Hattoria, T.; Miyanoa, S. *Tetrahedron Lett.* **2005**, *46*, 121; (e) Oueslati, I.; Thuéry, P.; Shkurenko, O.; Suwinska, K.; Harrowfield, J. M.; Abidie, R.; Vicensf, J. *Tetrahedron* **2007**, *63*, 62; (f) Bhalla, V.; Babu, J. N.; Kumar, M.; Hattorib, T.; Miyano, S. *Tetrahedron Lett.* **2007**, *48*, 1581.
36. Sheldrick, G. M. *SHELXS97, A Program for Crystal Structure Solution*; University of Göttingen: Göttingen, Germany, 1997.
37. Sheldrick, G. M. *SHELXL97, A Program for Crystal Structure Refinement*; University of Göttingen: Göttingen, Germany, 1997.